# THE CPS GAS-IONIZATION BEAM SCANNER

C.D. Johnson and L. Thorndahl
CERN, Geneva, Switzerland

## Summary

A non-destructive beam scanner was installed in the CPS ring early in 1968. Deriving a signal from the electrons liberated by the proton beam from the residual gas in the vacuum chamber and using a crossed electric and magnetic fields system of electron collection, the scanner gives the projected proton density distributions in the horizontal and vertical planes. Spatial resolution is better than 1 mm.

An important feature is the use of a single collector which receives electrons from a slice of the beam close to the zero equipotential surface. The electric equipotential surfaces are arranged to be parallel to the beam and scanning is achieved by displacing these equipotentials laterally in the region of the beam. In particular, the zero equipotential, which always passes through the detector, is scanned right through the beam.

Trials at scanning times down to 1 μS and normal CPS vacuum have yielded some interesting results. A double beam has been seen under certain conditions on the 'flat top' at 19 GeV/c, and other applications have been the study of beam dimensions during the first few ms after injection as well as debunching and slow ejection studies.

## Introduction

The number of electron-ion pairs generated per unit volume in a certain region of the proton beam is proportional to the proton density in that region. Fast collection of the electrons can provide a very convenient means of beam observation.

F. Hornstra and W. DeLuca[1] have used devices of the residual gas ionization type for beam observation in the ZGS of ANL. They have used an electric field to accelerate the ions or electrons onto a phosphor screen or a strip electrode system. Beam widths were several centimetres and no great demands were made on the spatial resolution of their devices.

In our case of a strong-focusing synchrotron we have more stringent requirements for spatial resolution. A strip-electrode system, combined with a focusing magnetic field (for electrons) along the direction of the electric field, could reasonably be used to provide a device having a spatial resolution of 1 or 2 mm. In order to cover the whole horizontal aperture of the CPS, 40 to 80 strips would be required and a suitable multiplexer system would have to be developed. The CPS Ionization Beam Scanner (IBS) has the necessary spatial resolution and avoids the multiplexer by collecting the electrons from the residual gas by a scanning system based on crossed electric and magnetic fields.

## Crossed Field Scanner

### General Features

The IBS is illustrated in Fig.1. Helmholtz coils give a region of uniform magnetic field, $\overline{B}$, in the beam direction. The electric field, $\overline{E}$, is provided by the two main electrodes $e_1$, $e_2$. Other electrodes connected to the main electrodes by a resistive and capacitive potential divider network are used to reduce fringe fields along the top and bottom gaps. The collector electrode is in the centre of the upper gap and at earth potential.

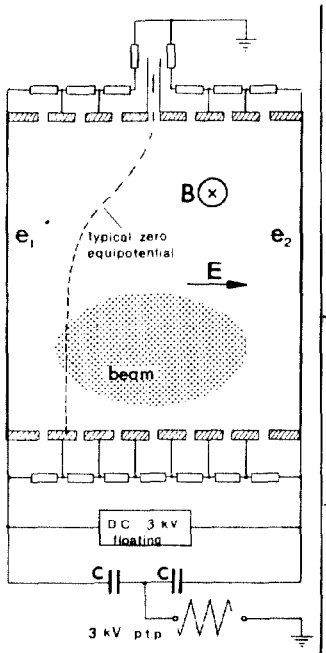


Fig. 1

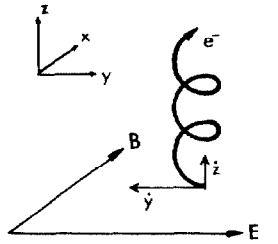


Fig. 2

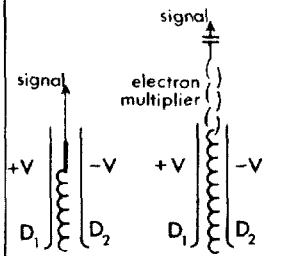


Fig. 3a Fig. 3b
IBS detectors

### Principle of Operation

In crossed uniform magnetic and electric fields trajectories of electrons will be cycloids which can be decomposed into a circular motion in the plane perpendicular to $\overline{E}$, with a radius:

$$R = \frac{(\dot{y}_o^2 + (\dot{z}_o - \frac{E}{B})^2)^{\frac{1}{2}}}{\frac{e}{m}B}$$

$\frac{e}{m}$ : electron charge to mass ratio

$\dot{y}_o$ : initial electron velocity component in the electric field direction

$\dot{z}_o$ : initial electron velocity component in the direction perpendicular to both the magnetic and electric fields

and a drift motion with the velocity $E/B$ in the z-direction, i.e. along electric equipotentials[2] (see Fig. 2).

In the case of non-uniform electric field, (still orthogonal to the uniform magnetic field) which results from the scanning (see Fig.1), we have assumed that for our choice of parameters the electrons will continue to drift along equipotential lines without any major change in R.

## Scanning Mechanism

Scanning is achieved by applying a triangular, or sine, waveform to the two main electrodes $e_1$, $e_2$ of Fig.1. In this way the equipotential surfaces are displaced laterally. In particular the earth equipotential surface, which always passes through the detector, can be scanned through the proton beam. The electrons arriving at the detector have been liberated and have travelled along or near to the earth equipotential. By careful arrangement of the electrodes an almost orthogonal projection of the beam is achieved. Field plotting in our case has shown that the equipotential surfaces in the region of the beam (shaded in Fig.1) are parallel within a few percent.

The electric equipotential surfaces can be perturbed by the space-charge potential of the beam, in particular at high intensities and small beam dimensions. This requires that the voltages applied to the device be large compared with the space charge potential. Its influence is in first order a position error; at present in the CPS this is a few millimetres. Future operation at high proton beam intensities will necessitate higher electric field strengths in the IBS in order to keep this error down to the same level.

Another requirement is that electric and magnetic fields be orthogonal over the region from which we collect ionization electrons, say 1% in our case, as otherwise these will be accelerated in the beam direction.

## Detector and Spatial Resolution

Two types have been studied. The first type was favoured initially, due to its simplicity. It essentially consists of three plates (see Fig.3a) where the centre plate aligned in the earth equipotential surface is the collector electrode and where the two outer plates, $D_1$, $D_2$, provide an electric field in the y-direction. This field is necessary to drift the electrons in the z-direction. The collection is based both on the circular as well as the drift motion of the electrons. The outer plates also act as collimators, preventing electrons of high initial energy, i.e. those moving with too large radii, R, from reaching the collector. The electrons passing through the detector mouth, without being collimated out, are electrons liberated in the potential interval whose upper and lower limits are given by the potentials of the plates $D_1$, $D_2$. This potential interval corresponds to a certain geometrical interval in the beam region. As collection onto the central electrode depends on the rotational motion, only electrons liberated in this geometrical interval can reach the collector. Electrons created slightly outside and having sufficient radius will hit the outer detector plates. The effective slit width is therefore approximately:

$$\text{separation of electrodes } e_1, e_2 \times \frac{\text{voltage between plates } D_1, D_2}{\text{voltage between electrodes } e_1 e_2}$$

We estimate the spatial resolution for our range of parameters to be a little less than the effective slit width. The second type of detector, (see Fig.3b) uses the first dynode of an electron multiplier as a collector. Both detectors have the interesting property that the effective slit width and so the spatial resolution can be varied from the control room by varying a voltage.

## Sensitivity and Scanning Time

With $10^{12}$ circulating protons in the CPS at a nominal pressure reading of $2\times10^{-6}$ Torr, we find that the ionization produced over a length of 10 cm in the beam direction gives sufficient signal to observe the beam by direct electron collection at scanning times down to 100 μS. The electron multiplier has improved the sensitivity by a factor of 100, giving a 1 μS scanning time, despite the fact that the collection efficiency is not 100% and that the collection length is reduced to 1 cm in the proton beam direction (due to the small size of the first dynode of the electron multiplier).

Thus, in its present state of development the IBS can scan through the proton beam in 1 μS at $2\times10^{-6}$ Torr of $N_2$. This performance exceeds our previous expectations[3] and may itself be bettered with improvements in the electron multiplier system. The final limit to the scanning speed appears to be that due to the time of flight of the electrons, which is 50 - 100 ns (see parameter list). This collection time should be short compared with the scanning time.

## Parameter List

| | |
|---|---|
| Separation between main electrodes: | 16 cm |
| Longitudinal dimension of electrodes: | 50 cm |
| Average collection distance for electrons: | 15 cm |
| Electric field between main electrodes: | 200 V/cm |
| Magnetic field B: | 100 - 150 Gauss |
| Average electron collection time: | 50 - 100 nsec |
| Detector mouth aperture: | 6 mm |

# The CPS Prototype

## Mechanical Construction

The IBS hardware is illustrated by Fig. 4, a view of the electrode system. The resistance-capacitance potential dividers are on the outside of the vacuum chamber. Electrical connections to the electrodes are made via their aluminium supports, which in Fig. 4 are just visible where they emerge from the ceramic insulators, S.

Outside the vacuum chamber are mounted two pairs of Helmholtz coils. Around the coils is a combined μ-metal and soft iron shield against fringe fields from the CPS magnets and also to improve the longitudinal magnetic fields within the IBS.

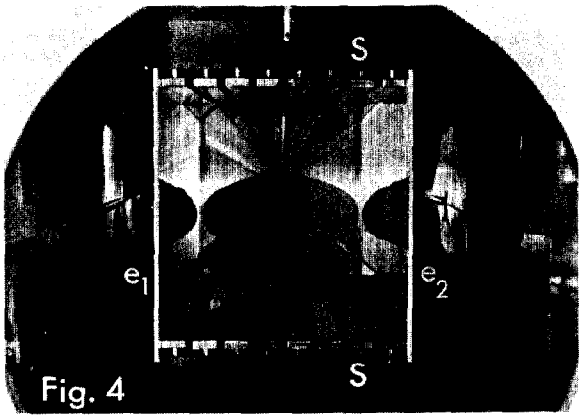

Fig. 4

Electronics

The major item of the electronics is the scanning voltage generator. At present, scanning frequencies up to 20 kHz are achieved using a Wavetek waveform generator and a high-voltage 150 W amplifier. Fast sweeps are made using triggered L-C ringing circuits of fixed frequencies. Signals are amplified by a transistor pre-amplifier of low output impedance, mounted directly onto the detector and a main amplifier located nearby in a region of low radiation. The overall voltage gain is 250 and the bandwidth dc to 10 MHz.

## Experimental Results

The prototype IBS has been in straight section 12 of the CPS since Easter 1968. The fast scan facility was developed very recently and is still being perfected.

The radial position indication given by the horizontal IBS has been compared with that obtained from induction electrodes and internal targets. A shift in radial position can be measured to within 1 mm. Absolute position measurements, after correction for the space charge potential effect, are in error by an amount corresponding to the difference in impedance between the plates $e_1$ and $e_2$ (Fig.1) and earth. The use of precision components in the potential divider chains should reduce this error to 1 mm.

Spatial resolution has been checked in the laboratory using thin tungsten filaments and a narrow electron beam to simulate the proton beam. The spatial resolution is found to depend as expected on the voltage applied across the detector plates and the highest resolution is such that true beam profiles are made wider instrumentally by less than 1 mm. A good check of this claim was made recently in collaboration with E. Brouzet. A 24 GeV/c bunched proton beam was set up on the 'flat top' of the CPS magnet cycle. A fork target having 10 mm internal separation between the vertical prongs of the fork was centered with respect to the beam (by minimizing target interactions). The IBS indicated a horizontal beam full width of 10 to 11 mm with the fork in position.

In the following photographs, which illustrate the many possible uses of the IBS, note that the IBS signal has been inverted to give positive profiles. The raster displays always start at the top of the picture and run downwards. A monitor signal of the scanning voltage taken directly from the IBS provides the horizontal deflection of the raster, which can thus be calibrated to correspond to position within the device. Except where otherwise stated, the horizontal scale of the displays is: 1 large division on the photograph is equal to 20 mm within the CPS and for the radial displays the right-hand side of the raster corresponds to the inside of the CPS ring.

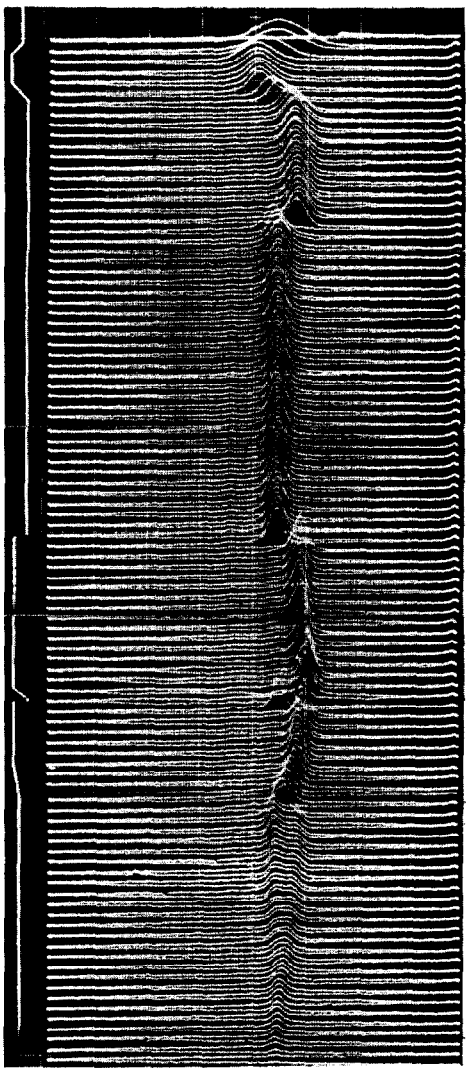


Fig. 5. A radial display of the full cycle of operation of the CPS. The trace running along the edge of the photograph is the RF radial shift control voltage and the corresponding beam movement can be seen. Note the change in sense of these shifts after transition, and the double beam, formed during the debunching, which is present during target 1 and 8 operation. The vertical scale is: 1 large division = 50 ms.

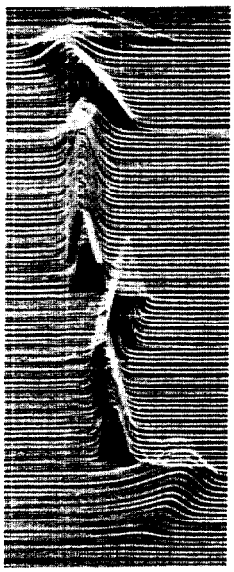

Fig. 6. A radial display of a machine operation ending with slow ejection from straight section 62. Note the asymmetrical profile during the slow ejection spill-out and the large radial position shift that marks the beginning of the ejection. In this photograph one large horizontal division = 15 mm within the CPS. Vertical time scale: 1 large division = 100 ms

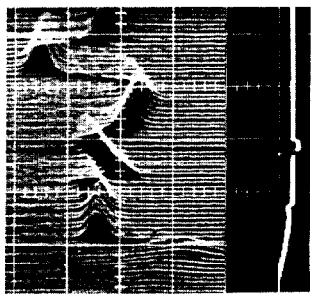

Fig. 7. Beam gymnastics at high energy. Target 6 operation during acceleration at 21 GeV/c, fast ejection from ss 58 on a 'flat top' at 24 GeV/c, followed by slow ejection from ss 62 on a second magnetic 'flat top' at 19.2 GeV/c, were responsible for the many radial position shifts in this photograph. The trace on the side of the photo is the magnetic 'flat top' monitor. Vertical time scale: 1 large division = 100 ms.

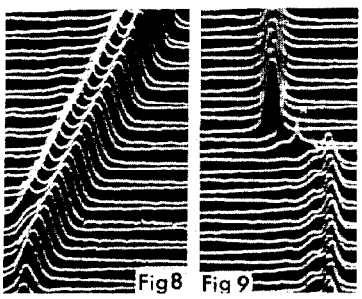


Fig. 8. A radial profile of a well defined double beam produced by misadjusting the debunching operation at the start of the magnetic 'flat top' at 19.2 GeV/c. A negative slope on the flat top sends the double beam across to the outside of the vacuum chamber where it is eventually lost against the chamber wall. Vertical time scale: 10 ms between scans.

Fig. 9. Another rather rare example of a double beam on the 'flat top' at high energy with RF (no debunching). The exact machine conditions which cause this splitting are not known. H.G. Hereward (private communication) has suggested that one beam is the normal bunched beam while the second beam, with slightly different energy, and therefore radius, has escaped from the bunches and is coasting alongside. Vertical time scale: 10 ms between scans.

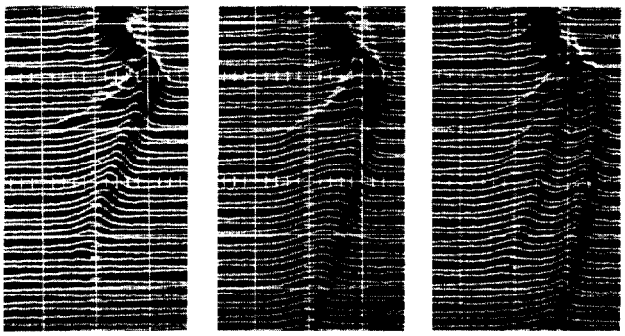

Fig. 10. Radial profiles during slow ejection spill-out tests at 24 GeV/c. These photographs show the variety of profiles which may be observed during the setting-up of a slow ejection operation. The normal smooth asymmetric profile of slow ejection shown in Fig. 6 has, in these examples, become broken up into two, three or even four separated beams. Vertical time scale: 1 large division = 25 ms.

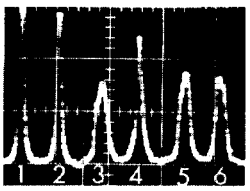


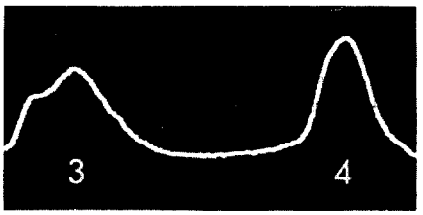


Fig. 11. Radial beam profiles just before, during and just after the debunching operation which precedes slow ejection. Profiles 1 and 2 are normal high-energy profiles, the beam full width being about 15 mm. Profile 3 has become wider, with a suggestion of being a double beam. Profile 4, 0.8 ms later, is again narrow, while a few ms later still the profiles 5 and 6 have become wide, as they remain for the whole of the slow ejection (cf. Figs. 6 and 8). The second photograph shows profiles 3 and 4 on an expanded time scale. These beam size observations can be explained in terms of the theory of the debunching operation.

The two photographs which follow are the first ones to be presented which have been made using the IBS with an electron multiplier as detector. The bandwidth of the system extends up to 10 MHz and so as we now can see the RF structure of the beam as an intensity modulation on the beam profiles, some explanation of the information contained in these profiles is required. In the CPS the RF is the 20th harmonic of the revolution frequency. The latter is about 150 kHz at injection and 500 kHz at high energy. Consider a profile obtained by scanning through the CPS beam in a time of 15 μS just after injection when the bunches are forming. The result will be as shown in Fig. 12.


Fig. 12. Example of a wide-band IBS profile just after injection.

In Fig. 12 the upper envelope is the profile which we normally associate with the IBS. This profile is modulated by the bunches. Also, due to incomplete filling, there is a 100% modulation at the revolution frequency (points $T_1$, $T_2$), i.e. we see the tail of the beam. Elsewhere the modulation is less than 100% due to the bunches being incomplete. The lower envelope therefore, gives the dc profile, or the profile of the unbunched portion of the beam. This may not correspond exactly to that of the bunched portion. As acceleration proceeds and the bunches are completed, the 3 MHz modulation becomes 100%. During debunching the reverse occurs and again the beam profiles can be separated into bunched and unbunched portions.

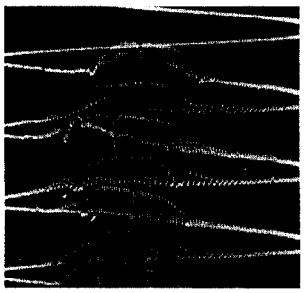

Fig. 13 is an example of injection at a scanning frequency of 10 kHz (due to a fault in the scanning voltage amplifier the scanning waveform is slightly distorted, giving a faster scan from right to left than from left to right). As described above, the bunch structure is clearly seen as is the 100% modulation due to the 'tail' of the beam. Injection is several μS before the first scan and the bunches are already forming as this scan is made. 300 μS later the bunches are fully formed. Note that the unbunched portion of the beam drifts towards the inside of the CPS ring (the left-hand side of this photograph) as acceleration proceeds. Note also the beam blow-up which occurs between the first and second scans.

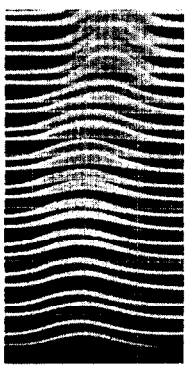

Fig. 14 is another example of a 10 MHz bandwidth photograph, this time of the debunching operation which precedes target 1 operation. Note the fully bunched (100% modulated) profile at the top of the photograph and the progressive debunching to the fully debunched beam at the bottom. There is a slight radial position shift and a 20% increase in beam size (radially). The vertical time scale is: 1 ms between scans and the horizontal scale is approximately 1 large division = 5 mm within the IBS.

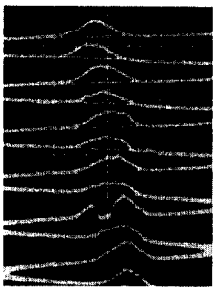

Fig. 15 shows horizontal profiles just after injection without acceleration (no bunches). Note the intensity modulation of profile No. 9 due to the tail of the beam. The beam spirals to the inside of the vacuum chamber as the magnetic field rises.

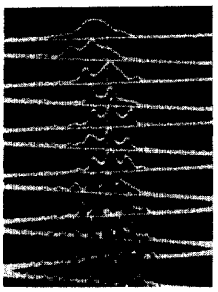

Fig. 16 was taken under the same conditions but with acceleration. Time between scans is 15 μS, the time for the first scan through the beam is 1 μS. This increases as the amplitude of the scanning voltage decreases (ringing circuit). Horizontal scale: 1 large division = 4 cm in the CPS.

## Conclusions

With the last two photographs we appear to have reached the ultimate scanning speed of the IBS. There is some interest to go faster for observation of the unbunched beam after injection, but for a bunched beam greater speed is pointless, since the intensity modulation due to the bunches spoils the profiles. One would have to scan in a time short compared to the bunch length, e.g. 1 ns, in order to obtain good profiles of single bunches. This is beyond the capabilities of the IBS.

With reduced scanning times, e.g. 100 μS, the use of an electron multiplier means that it is feasible to operate an IBS at pressures of $10^{-8}$ Torr, with $10^{12}$ circulating protons and a collection length of only 1 cm.

At low scanning speeds, the IBS, with a raster display, proves to be a most convenient operational method for observing, in an immediately available analog form, the beam position and size during the whole of the machine cycle.

We are grateful for the support which has been given to this work by the ISR and MPS Divisions of CERN, to the many people who have assisted with the development and trials of the prototype, to Mr. W. Saint-Aubert for his considerable technical assistance and to Mrs. J. Eddison for her assistance in preparing this manuscript.

## References

1. HORNSTRA, F. and DELUCA, W.H., Non-destructive beam profile detection systems for the ZGS, ANL internal report, 1967

2. BLANC-LAPIERRE, A., GOUDET, G., LAPOSTOLLE, P., Electronique générale, Eyrolles, Paris, 1953, pp. 247-249

3. JOHNSON, C.D., THORNDAHL, L., CERN internal report, MPS/Int.CO 68-13